



Blood Flow Simulation in an Aorta with a Mild Coarctation using Magnetic Resonance Angiography and Finite Volume Method

R. Ghasemiasl*, R. Ostadhossein, M. A. Javadi, S. Hoseinzadeh

Department of Mechanical Engineering, West Tehran Branch, Islamic Azad University, Tehran, Iran

PAPER INFO

Paper history:

Received 23 September 2017

Received in revised form 01 December 2017

Accepted 21 December 2017

Keywords:

Aortic Coarctation

Finite Volume Method

Magnetic Resonance Angiography

Large Eddy Simulation Model

Windkessel Model

ABSTRACT

Coarctation of the aorta is one of the five main congenital cardiovascular failures, accounting for 6–8 percent of these failures. This research aimed to simulate the blood flow of a seventeen-year-old male teen with a mild coarctation at one-third of his aorta's descending branch. The simulation was performed by extracting the domain and the input pulsatile velocity signal as the boundary condition at the aorta entrance using magnetic resonance angiography (MRA) and the finite volume method (FVM), as well as a large eddy simulation (LES) turbulence model. The results were validated by comparing the blood flow static pressure from the numerical simulation to a clinical measurement available in the literature. The inclusion of the turbulence model in the solution resulted in a static pressure for the heart's normal function at the coarctation that agreed very well with the clinical measurement; the difference was just 0.39 mmHg. Therefore, the study confirmed the validity of the simulation results, the assumption that a turbulence regime exists inside an aorta with a coarctation, and the efficiency of the LES turbulence model for simulating cardiovascular flows.

doi: 10.5829/ije.2018.31.04a.20

1. INTRODUCTION

Coarctation of the aorta (CoA), first studied in 1760 by Morgagni [1], occurs typically in about 0.4% of live births and accounts for an average of 7% of congenital cardiovascular failures. Jain et al. [2] offered a mathematical model of blood flow in a stenosed artery considering the MHD effect through the porous medium. Kumar et al. [3] investigated oscillatory MHD blood flow through an artery with mild stenosis. Jain et al. [4] offered a mathematical model for blood flow through narrow vessels with mild stenosis. Gupta [5] offered a model to analyze blood flow in small vessels with magnetic effects. Crosetto et al. [6] used fluid-structure interaction (FSI) to conduct a numerical simulation based on a few cardio cycles as the inlet boundary conditions. Jahangiri and Saghafian [7] used standard K- and RNG K- ϵ turbulence models and entered the elastic properties of the artery wall into the problem to simulate the turbulent flow passing through

a CoA. They found good agreement between their solutions obtained from the standard K- ϵ turbulence model and values reported in the literature [7]. Yin et al. [8] discovered a somewhat severe pressure gradient at the aorta arc through their simulation. Manimaran [9] reported a non-Newtonian blood flow passing through an arterial stenosis with surface irregularities. Wang et al. [10] investigated the blood flow properties at the aortic coarctation of a male teen while assuming an existing laminar Newtonian flow along the rigid artery wall. Sotelo et al. [11] researched for the quantification of wall shear stress using a finite-element method in multidimensional phase-contrast MR data of the thoracic aorta. Arokiara et al. [12] designed a stent without the stent graft and the stent was deployed by an endovascular method in a virtual patient-specific aneurysm model. The stress-strain analysis and deployment characteristics were performed in a finite element analysis using the Abaqus software [12]. This paper includes a simulation of blood flow on a seventeen-year-old male with a mild coarctation using Large Eddy Simulation method to simulate the

*Corresponding Author's Email: ghasemiasl.r@wtiau.ac.ir (R. Ghasemiasl)

turbulence blood flow at the restriction zone by employing Finite Volume Method to solve the governing equations. The results show a perfect agreement with the test results gaining from MRA in the literature.

2. METHOD AND RESULTS

2. 1. The Physical Specification of the Patient and the Solution Domain

The investigated case was a seventeen-year-old male teen with a mild coarctation in one-third of the descending branch. The patient weighed 71 kilograms, was 177 centimeters tall, and had a surface area of 1.9 square meters. The time difference between his two cardiac cycles at the normal cardiac function was 1.277 seconds. The following equation:

$$f = \frac{1}{T} \quad (1)$$

gives a frequency for this cardiac cycle of 0.783 Hertz; where T is the time difference in seconds between two consecutive cardiac cycles and f is the frequency of each cycle in Hertz.

The magnetic resonance angiography (MRA) was performed with a Philips scanner with a 1.5 Tesla magnetic field, using gadolinium-based Dotarem (gadoterate meglumine) as the contrast agent. The extracted domain from the MRA contained the ascending branch, the arc, the descending branch of a aorta, and the three facial branches. The domain was extracted with 69286 nodes and 138532 surfaces in Stereolithography (STL) format². Figure 1 illustrates the domain inlet and outlets. Figure 2 shows the restriction in one-third of the descending branch.

2. 2. Governing Equations The pulsatile flow in this simulation considered to be an incompressible Newtonian viscous flow. The density was assumed to be 1000 kg/m³ and the viscosity was considered to be 0.004 Pa.s. The continuity and Navier-Stokes equations were applied as the primary governing equations of this simulation.



Figure 1. The domain inlet and outlets

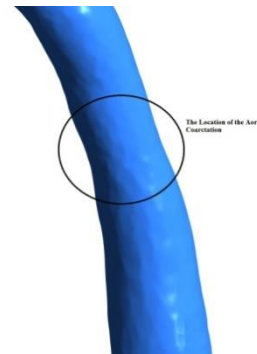


Figure 2. The restriction in one third of the descending branch

$$\vec{\nabla} \cdot \vec{u} = 0 \quad (2)$$

$$\frac{\partial \vec{u}}{\partial t} + (\vec{\nabla} \cdot \vec{u}) \vec{u} = -\frac{1}{\rho} \vec{\nabla} P + \nu \nabla^2 \vec{u} + \vec{F} \quad (3)$$

Where u is the velocity of blood flow, ν is kinematic viscosity, ρ is the density of blood, P is the dynamic pressure, and F is the subjected body forces, which is mainly gravity here in this problem. The fluctuations existing inside the blood flow during the implementation of the solution procedure were simulated by applying the large eddy simulation (LES) turbulence model. The Navier-Stokes equation was filtered through this model and only the fluctuations considerably larger than the mesh size was directly solved. The eddies not considerably larger were processed using a sub-grid scale (SGS) turbulence model. The turbulence viscosity of the SGS model was simulated using the equation proposed by Smagorinsky and Lilly[13] with a coefficient of 0.2.

2. 3. Artery Wall In this problem, the flexibility of the artery was ignored, and the artery wall was assumed rigid.

2. 4. Boundry Conditions In solving this problem, a no-slip condition was imposed on the artery wall. The pulsatile mass flow rate signal from MRA was driven by sampling eighty-three pieces of data at 0.016-second increments. The pulsatile velocity signal as the input boundary condition was driven by the mass flow rate signal based on the density of blood and the cross-section area of the aorta inlet, which was 21.39 millimeters. The associated signals were mathematically modeled using the eight first terms of relevant Fourier series, according to the repetitive nature of cardiovascular cycles. Figure 3 shows the input cardiovascular signal.

²www. www.vascularmodel.org/miccai2013

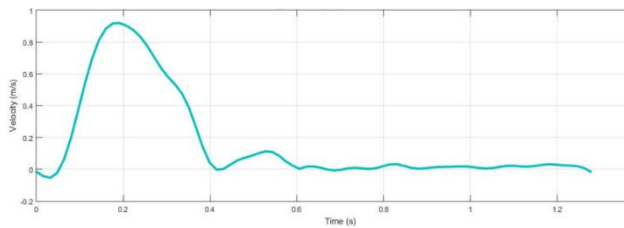


Figure 3. The input cardiovascular signal

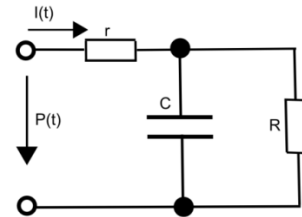


Figure 4. The three-element Winkessel Model schema

A shortage of data at the aorta outlets led to the design of a three-element Winkessel Model to predict the static pressure at each outlet [14]. The model consists of a resistor to include the hydraulic resistance of the aorta along the flow, a capacitor to model the elastic properties of the wall, and a second resistor to involve the apparent resistance of the aorta. A schema of this model is depicted in Figure 4.

The governing differential equation of the Winkessel Model is in the form:

$$(1 + \frac{r}{R})I(t) + Cr \frac{dI(t)}{dt} = \frac{P(t)}{R} + C \frac{dP(t)}{dt} \tag{4}$$

Where t represents time, R and r both introduce the magnitude of the resistors to the model, C indicates the capacity of the relevant capacitor, I(t) shows the input pulsatile mass flow rate, and P(t) represents the pulsatile static pressure at the outlets. Including the pulsatile mass flow rate signal in the equation and assigning the share of each output from the total input mass flow rate resulted in a pulsatile signal for the static pressure for each output. The internal diameter and the portion of each output from the input mass flow rate, as well as the numerical values of the Winkessel parameters, are listed in Tables 1, 2, and 3, respectively.

In this research, the Runge-Kutta 4th, order method was applied to solve Equation (4) and a FORTRAN piece of code was written to implement and achieve the results.

The pulsatile pressure signals for each output were mathematically modeled separately by determining the eight first terms of the associated Fourier series. Figure 5 shows the static pressure signal for output 1.

TABLE 1. Diameters of the aorta's outlets in millimeter

Outlet	Outlet 1	Outlet 2	Outlet 3	Outlet 4
Diameter (mm)	12.84	5.98	3.61	7.81

TABLE 2. The share of each output from the input mass flow rate in percent

Output	Output 1	Output 2	Output 3	Output 4
Share (%)	12.84	5.98	3.61	7.81

TABLE 3. The magnitude of the Winkessel parameters

Element	Outlet 1	Outlet 2	Outlet 3	Outlet 4
R	1.42×10^7	1.59×10^8	5.98×10^7	1.37×10^7
C	3.45×10^{-9}	1.60×10^{-9}	2.11×10^{-9}	1.68×10^{-8}
R	5.87×10^8	1.31×10^9	1.47×10^9	2.12×10^8

Instability of the result signals during the initial seconds was circumvented by applying the solutions 25 seconds after the start to drive the Fourier series. All signals were utterly stable by that time.

2.5. Mesh Generation The meshes were generated using the free mesh generation code NETGEN, which is capable of generating a tetrahedral mesh. The mesh independence of the problem was tested by creating three different mesh structures of various sizes. The specifications of each mesh, including the number of nodes and elements, are summarized in Table 4.

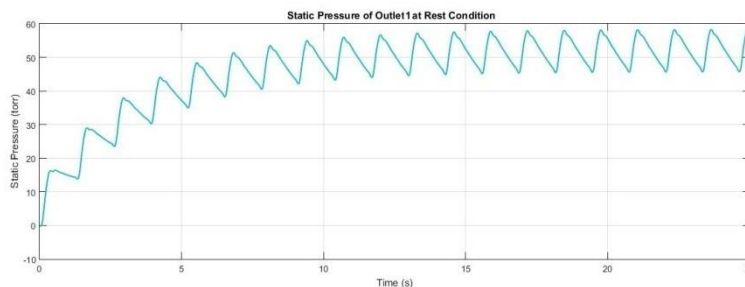


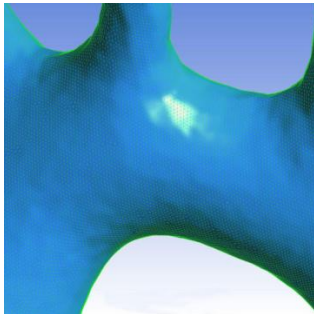
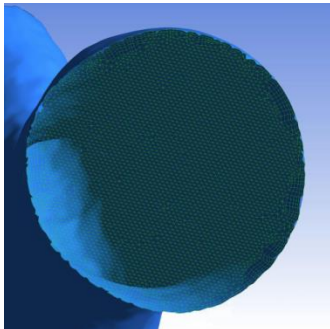
Figure 5. The static pressure signal for output 1

TABLE 4. The number of nodes, trihedral and tetrahedral elements within the mesh

Mesh	Number of Nods	Number of Trihedral Elements	Number of Tetrahedral Elements
Coarse	388295	1195456	425851
Fine	1365789	2985632	1335874
Very Fine	2191326	3894422	2492645

Figure 6 illustrates the generated mesh on the surface of the aorta and Figure 7 indicates the generated mesh at the aorta entrance.

2.6. Accomplishment The statistical approach taken in this paper to obtain velocity and pressure fields at the aortic coarctation was the Finite Volume Method (FVM). The SIMPLE algorithm, along with the free code Open FOAM, was applied to implement the FVM. Each time step was considered to be 0.01 seconds, and the accuracy of the convergence of the relevant parameters was chosen as 0.001. The maximum number of iterations was selected as 100 and solutions were extracted at the peak of the input mass flow rate and velocity signals, which was 0.19 seconds after the start. The results were validated by comparing the difference between the average static pressure at the upstream and the downstream of the coarctation to the value reported by Wang et al. [10].

**Figure 6.** The generated mesh on the surface of the aorta**Figure 7.** The generated mesh at the aorta entrance

3. DISCUSSION

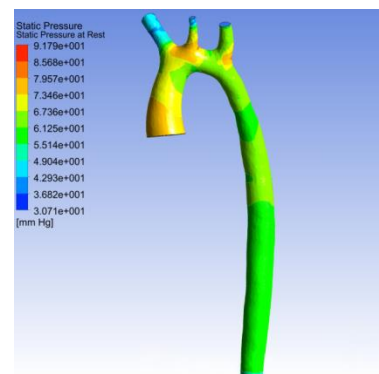
The correctness of the mesh-independency assumption was validated by comparing the driven numerical results of the velocity and average static pressure at the coarctation obtained from the three generated meshes. Table 5 shows the results associated with the velocity and average static pressure at the coarctation within these types of meshes.

The results obtained with the fine and very fine meshes show that the velocity and average static pressure in both meshes are close in magnitude; thereby verifying the mesh-independency assumption. Ultimately, the results using the very fine mesh were utilized to reveal the blood flow properties. Figure 8 shows the static pressure field of the blood flow passing through the aortic coarctation. A pressure gradient is evident at the coarctation, with the average static pressure at this position equal to 58.195 mmHg. The maximum static pressure occurs at the entrance, where the magnitude is 91.8 mmHg. The minimum static pressure is seen at the cerebral and facial outputs, which agrees with the physiologic facts. The difference in the average static pressure magnitude at both sides of the coarctation is 0.39 mmHg. This amount of error demonstrates the advantage of the present simulation over the simulation previously performed by Wang et al. [10].

Figure 9 shows the velocity of the flow through the aorta, which equals 1.71 m/s at the center of the coarctation.

TABLE 5. The results for the velocity and static pressure at the coarctation

Mesh	Static Pressure (mm Hg)	Mean Velocity
Coarse	47.805	0.65
Fine	57.625	1.73
Very Fine	58.195	1.71

**Figure 8.** The static pressure field of the blood flow passing through the aortic coarctation

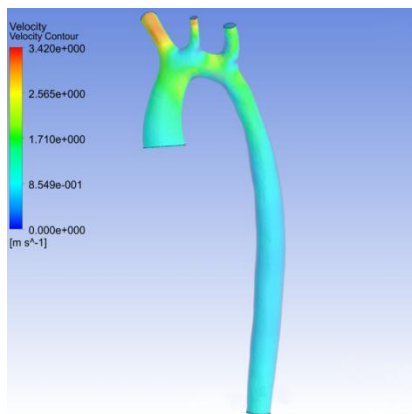


Figure 9. The velocity of the flow through the aorta

The maximum velocity is available at inlets 3, and 4 and the magnitude is 3.42 m/s. The maximum velocity is seen at the inlet.

4. CONCLUSION

The findings presented here confirm that the LES model is capable of simulating the fluctuations caused by coarctation. Application of a three-element Winkessel model with appropriate coefficients as the static pressure predictor at the aorta outlets can produce a pulsatile static pressure signal with acceptable accuracy, thereby permitting the simulation of blood flow for the investigation of various types of cardiovascular diseases.

5. REFERENCES

- Morgagni, J., "De sedibus et causis morborum, 1761", *Classics of cardiology. Malabar, Fla: Robert E. Kreiger*, (1983), 186-187.
- Jain, M., Sharma, G. and Singh, R., "Mathematical modelling of blood flow in a stenosed artery under mhd effect through porous medium", *International Journal of Engineering, Transactions B*, Vol. 23, No. 3-4, (2010), 243-251.
- Kumar, S. and Kumar, D., "Oscillatory mhd flow of blood through an artery with mild stenosis (research note)", *International Journal of Engineering-Transactions A: Basics*, Vol. 22, No. 2, (2008), 125-130.
- Jain, M., Sharma, G. and Sharma, S.K., "A mathematical model for blood flow through narrow vessels with mild stenosis", *International Journal of Engineering, Transactions B: Applications*, Vol. 22, No. 1, (2009), 99-106.
- Gupta, A.K., "Performance model and analysis of blood flow in small vessels with magnetic effects", *International Journal of Engineering-Transactions A: Basics*, Vol. 25, No. 2, (2012), 189-196.
- Crosetto, P., Reymond, P., Deparis, S., Kontaxakis, D., Stergiopoulos, N. and Quarteroni, A., "Fluid-structure interaction simulation of aortic blood flow", *Computers & Fluids*, Vol. 43, No. 1, (2011), 46-57.
- Jahangiri, M., Saghafian, M. and Sadeghi, M.R., "Numerical study of turbulent pulsatile blood flow through stenosed artery using fluid-solid interaction", *Computational and Mathematical Methods in Medicine*, Vol. 2015, (2015), Article ID 515613.
- Yin, J., Xiang, Y. and Dou, Q., "Three-dimensional reconstruction and numerical simulation of blood flow in human thoracic aortic", in *Bioinformatics and Biomedical Engineering (iCBBE), 2010 4th International Conference on, IEEE.*, (2010), 1-4.
- Manimaran, R., "Cfd simulation of non-newtonian fluid flow in arterial stenoses with surface irregularities", *World Academy of Science, Engineering and Technology*, Vol. 73, No. 5, (2011), 804-809.
- Wang, X., Walters, D.K., Burgreen, G.W. and Thompson, D.S., "Traditional cfd boundary conditions applied to blood analog flow through a patient-specific aortic coarctation", in *International Workshop on Statistical Atlases and Computational Models of the Heart, Springer.*, (2013), 118-125.
- Sotelo, J., Urbina, J., Valverde, I., Tejos, C., Irarrázaval, P., Hurtado, D.E. and Uribe, S., "Quantification of wall shear stress using a finite-element method in multidimensional phase-contrast mr data of the thoracic aorta", *Journal of Biomechanics*, Vol. 48, No. 10, (2015), 1817-1827.
- Arokiaraj, M., De Beule, M. and De Santis, G., "A novel sax-stent method in treatment of ascending aorta and aortic arch aneurysms evaluated by finite element simulations", *JMV-Journal de Médecine Vasculaire*, Vol. 42, No. 1, (2017), 39-45.
- Lilly, D.K., "A proposed modification of the germano subgrid-scale closure method", *Physics of Fluids A: Fluid Dynamics*, Vol. 4, No. 3, (1992), 633-635.
- Westerhof, N., Lankhaar, J.-W. and Westerhof, B.E., "The arterial windkessel", *Medical & Biological Engineering & Computing*, Vol. 47, No. 2, (2009), 131-141.

Blood Flow Simulation in an Aorta with a mild coarctation Using Magnetic Resonance Angiography and Finite Volume Method

R. Ghasemiasl, R. Ostadhossein, M. A. Javadi, S. Hoseinzadeh

Department of Mechanical Engineering, West Tehran Branch, Islamic Azad University, Tehran, Iran

PAPER INFO

چکیده

Paper history:

Received 23 September 2017

Received in revised form 01 December 2017

Accepted 21 December 2017

Keywords:

Aortic Coarctation

Finite Volume Method

Magnetic Resonance Angiography

Large Eddy Simulation Model

Windkessel Model

انسداد مادرزادی آئورت یکی از پنج نقص قلبی مادرزادی است که 6 تا 8 درصد کلیه نقایص قلبی-عروقی را شامل می شود. هدف از این تحقیق شبیه سازی جریان خون در یک نوجوان هفده ساله مذکر به همراه یک گرفتگی ملایم در یک سوم شاخه صعودی آئورت می باشد. شبیه سازی مورد نظر از طریق استخراج مدل و سیگنال سرعت نوسانی ورودی به عنوان شرط مرزی مسئله در ورودی آئورت با استفاده از آنژیوگرافی رزونانس مغناطیسی و روش حجم محدود به همراه مدل شبیه ساز آشفتگی گردابه های بزرگ انجام پذیرفته است. نتایج این پژوهش از طریق مقایسه فشار استاتیک به دست آمده از شبیه سازی عددی و اندازه گیری بالینی موجود پیشینه پژوهش به انجام رسیده است. نتایج حاصل از شبیه سازی فشار استاتیکی به همراه به کارگیری مدل آشفتگی مذکور انطباق بسیار خوبی را با اندازه گیری بالینی نشان می دهد. میزان اختلاف تنها 0/39 میلی متر جیوه می باشد. مقایسه مقادیر حاصل از شبیه سازی عددی و اندازه گیری بالینی فرض وجود یک جریان آشفتگی در موضع انسداد و کارایی مدل آشفتگی شبیه ساز گردابه های بزرگ را در شبیه سازی جریان های قلبی عروقی تایید می نماید.

doi: 10.5829/ije.2018.31.04a.20